ICANS-XV
15th Meeting of the International Collaboration on Advanced
Neutron Sources
November 6-9, 2000
Tskuba, Japan

The SNS SuperConducting Linac Architecture

J. Galambos[1*], J. Stovall[2], S. Nath[2], H. Takeda[2], J. Billen[2], L.Young[2] , D. Jeon[2], J. Wei[2], K. Crandall[3]

[1]SNS-Oak Ridge National Laboratory
SNS-Los Alamos National Laboratory
[3]Tech Source Co., New Mexico
* email: galambosjd@ornl.gov

Abstract

A new Spallation Neutron Source (SNS) is presently under construction at the Oak Ridge National Laboratory in Tennessee[1]. A conventional linac, accelerates a 52-mA beam to 186 MeV. The SRF linac accelerates the beam to 1.25 GeV using 117 elliptically shaped 6 cell cavities. Two cavity beta types are used, with geometrical betas of 0.61 and 0.81. This paper describes the optimization leading to the choice of cavity betas and number of different cavity types. Also, beam-dynamics throughout the entire linac are presented.

1. Introduction

The SNS super-conducting RF linac architecture choice is influenced by several requirements. First, the output energy should be $\geq$ 800 MeV in order to produce at least a 1 MW short pulsed beam to the neutron target. Sometime after the initial commissioning, with the benefit of additional cavity processing the linac is expected to produce a 1300 MeV beam, so there is a range of operational energies the linac needs to perform well in. Additional considerations guiding the choice of cavity beta include the maximum phase slip, and the minimum transit time factor (TTF) of the first cavity at the transition between the high and low beta sections. If the transit time factor is too small (or the phase slip too large) there is a danger of not accelerating the beam should the cavity accelerating gradient be lower than expected. The choice of the first superconducting cavity beta also needs to match the energy out of the warm CCL structure, and project cost and schedule constraints limit the number cavity beta types that can be used. Consideration of these issues leads to the SNS baseline of a medium beta cavity section of 11 cryo-modules with a geometrical beta (b_g) of 0.61 and a high beta cavity section using b_g = 0.81 and up to 21 cryo-modules. The optimizations leading to these choices are discussed in the following Section II. Some beam dynamics are shown in Section III.

II. Choice of Cavity Beta

The super-conducting cavity geometric beta (β_g) is picked to maximize the beam acceleration for the conditions expected to be achieved in the SNS. Factors influencing the optimization include the incoming beam energy, the cavity accelerating gradients, the number of cryo-modules for each cavity beta type, and the number of superconducting cavity types. Only two superconducting cavity types are used here, in large part due to timing considerations, as project schedule constraints permit the prototyping of only two cavity types. For SNS the beam energy at the entrance to the superconducting section is taken to be 187 MeV. The design of the warm section of the SNS linac is already fairly mature, and 187 MeV is the exit energy from the 4th CCL module, which is at a breakpoint for RF partitioning. Some of these conditions and other modeling assumptions are listed in Table 1. Regarding nomenclature, in the SNS, the first cavity beta section is referred to as the medium beta section and the second cavity beta section is referred to as the high beta section. The model used for these studies is a simple synchronous particle acceleration model, which incorporates a cell-by-cell integration method [2].

Initially we consider b_g optimizations for the case of 11 medium beta cryo-modules with 3 cavities each, and 17 high beta cryo-modules with 4 cavities each. Additionally, we note that the linac tunnel is sized to accommodate up to 4 more high beta cryo-modules (for a total of 21 high beta cryo-modules).

Table 1. Partial list of assumptions used in the SNS cavity beta studies.

Phase law:	• Starting phase of the medium beta cryo-module family = 22^o, with a bilinear ramp to the final phase (2/3 phase change occurs in first 1/3 of family) • Phase of the high beta cryo-module = 26.5^o • Ending phase of the medium beta cryo-module is solved to give constant E_0 T sin(ϕ)b_g.
Peak surface field (E_{peak}):	27.5 MV/m
E_{peak} / E_0 (1):	$1/\left(-0.4814+2.244b_g+1.1129b_b^2\right)$
Number of cells/cavity:	6
Cavities/ cryo-module:	• 3 for medium beta cryo-module • 4 for medium beta cryo-module
Linac architecture:	• Two b_g families • Constant gradient / cavity

(1) – this is a fit of Superfish output of three similarly optimized cavities: b_g = 0.45 with E_{peak} / E_0 = 3.3, : b_g = 0.61 with E_{peak} / E_0 = 2.11, : b_g = 0.81 with E_{peak} / E_0 = 1.65

Figure 1 shows the final beam energy for various b_g values calculated using the reference peak surface field of 27.5 MV/m. The choice of medium beta cryo-module b_g has only a

small influence on the beam acceleration, with a marginal benefit going above b_g = 0.61. This insensitivity is largely due to the fixed entrance energy to the superconducting section. b_g = 0.61 is the SNS medium beta cryo-modules b_g value . The choice of b_g for the high beta cryomodule is more sensitive, with the maximum acceleration at nominal conditions occurring near b_g = 0.82. Using b_g = 0.82 instead of b_g = 0.76 offers an additional ~55 MeV acceleration for the nominal conditions. However, rather than pick the absolute optimum b_g value for the high beta section, we pick a slightly lower nominal value of 0.81, based on considerations discussed later.

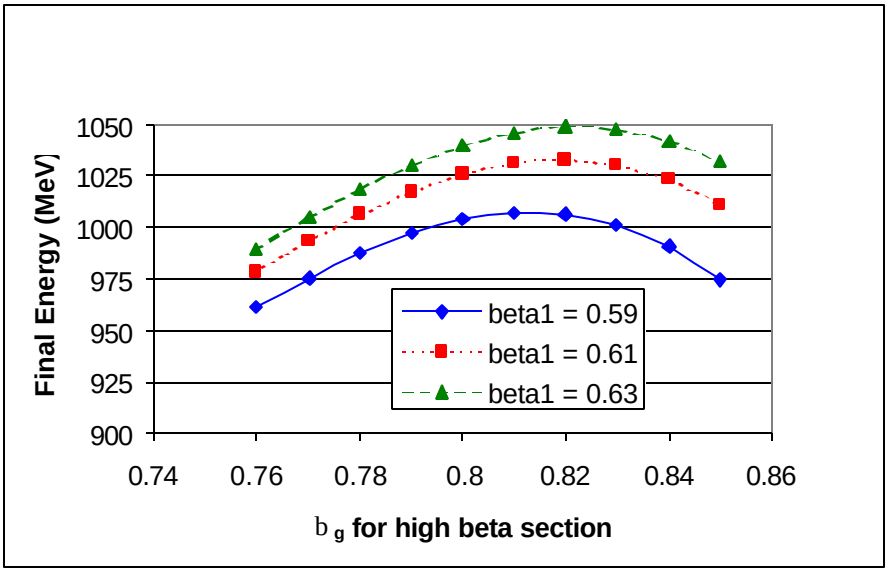

Figure 1. Final beam energy vs. the high beta cryomodule b_g, for three different medium beta cryomodule b_g values. The reference peak surface field of 27.5 MV/m is used here, with 11 medium beta cryo-modules and 17 high beta cryo-modules. .

Sensitivity to Lower Accelerating Gradients

One concern in picking the superconducting cavity beta is ensuring that the device will perform reasonably well, even in the event that accelerating gradients lower than expected are encountered. Figure 2 shows the attainable beam energy under conditions of reduced attainable accelerating gradient, namely with the peak surface field limited to 25 MV/m . Even with a reduced accelerating gradient there is still sufficient acceleration to reach a high enough energy at the transition between beta types to maintain acceleration. With 17 high beta cryo-modules, the attainable beam energy is 940 MeV, and with 21 cryo-modules the beam energy is about 1100 MeV. Providing the tunnel space for 21 high beta cryo-modules permits attaining greater than 1000 MeV even in the unlikely event of only achieving a peak surface field of 25 MV/m . Also, use of b_g = 0.81, as opposed to a higher value, tends to maximize the beam energy with a reduced accelerating gradient.

Sensitivity to Higher Accelerating Gradients

Improved performance using b_g =0.81 for the second section, instead of say b_g =0.76, is more pronounced if higher accelerating fields are assumed. This is evident in Figure 3, which

shows the final beam energy vs. b_g for the case of a peak surface field of 30 MV/m and 21 high beta cryo-modules are used. In this scenario, operation near 1300 MeV is achieved for b_g = 0.81, whereas only 1180 MeV is attained for b_g = 0.76.

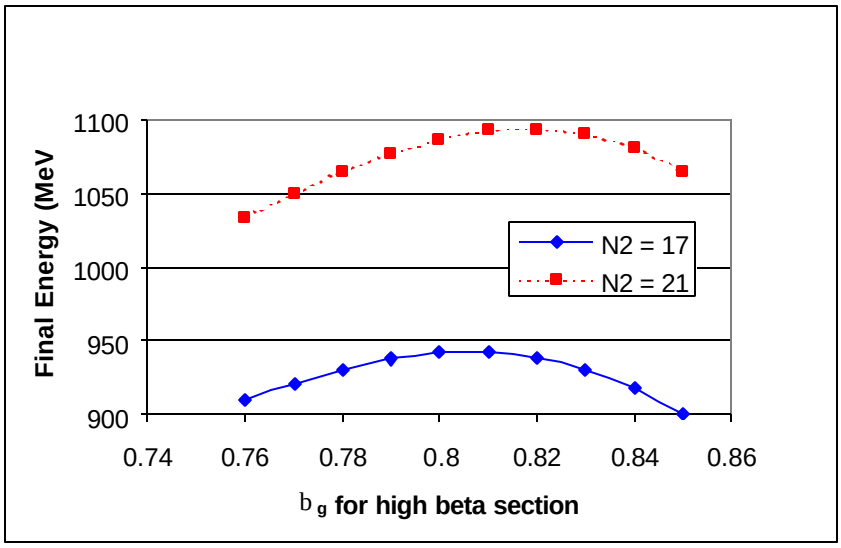

Figure 2. Final beam energy vs. the high beta cryomodule b_g, for 11 medium beta cryo-modules with b_g = 0.61, 17 and 21 high beta cryo modules, and a lower peak surface field of 25 MV/m.

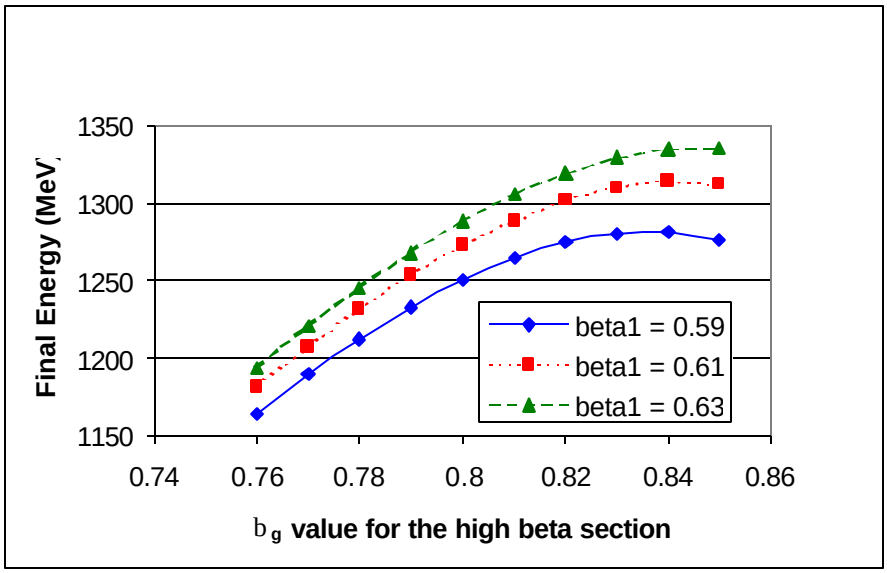

Figure 3. Final beam energy vs the high beta cryomodule β_g, for three different medium beta cryomodule β_g values. A peak surface field of 30 MV/m is used here.

III Number of Cryo-modules

The above analysis indicates that the choice of the medium beta cryomodule b_g is insensitive and that b_g = 0.61 is a good choice for the medium beta cryo-module section. Also the b_g for

the high beta cryo-module should be ~ 0.81. Here we investigate the impact of the number of medium and high beta cryo-modules. Figure 4 shows the attainable energy vs. the number of medium beta cryo-modules for three different values of the high beta cryo-module b_g. The total number of cryo-modules is held fixed at 28, so this study represents a trade-off between high beta and medium beta cryo-modules. As seen previously, increasing the high beta cryo-module b_g value is beneficial, although there is a diminishing benefit as b_g = 0.81 is approached. Also, going to fewer medium beta cryo-modules improves the energy gain of the linac.

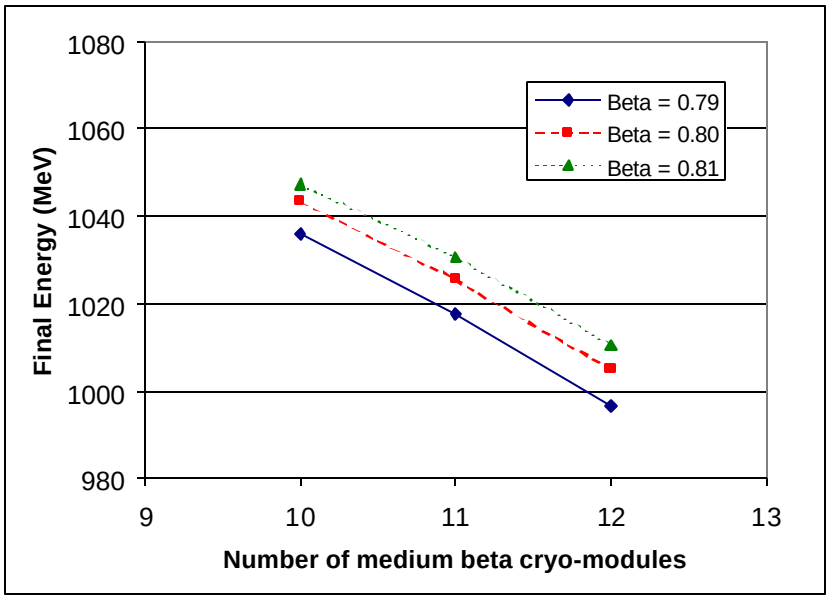

Figure 4. Final energy vs. the number of medium beta cryo-modules. The total number of cryo-odules is held fixed at 28, and the medium beta cryo-module β_g is 0.61.

However, additional considerations influence the choice of the number of medium and high beta cryo-modules. Figure 5 shows the maximum phase slip and minimum cavity transit time factor (TTF) at the first cavity in the high beta cryo-module section, where extremes to these quantities occur. The conditions that maximize the energy gain from the linac also lead to small TTF and large phase slip in the first high beta cavity. The low TTF level with fewer medium beta cryo-modules indicates that the transition energy is approaching the value below which, the high beta cavity will no longer accelerate the beam. While the simple synchronous particle model used here favors a fewer number of cryo-module to obtain the maximum energy gain, some allowance needs to be made for effects not included in this model. These additional effects include: (1) the phase spread of a real bunch, (2) machine imperfections, (3) operation with failed cavities, and (4) the possibility that the peak surface fields will be lower than the 27.5 MV/m assumed here.

Due to these additional considerations, the SNS design choice provides some allowance, and uses 11 medium beta cryo-modules with b_g = 0.61. The initial number of high beta cryo-modules is 15, due to cost considerations. However, room is provided to accommodate an additional 6 high beta cryo-modules in the tunnel. This parameter choice meets the cost constraints, provides initial operation near 1 GeV, provides some design margin in the physics at the transition region, and provides an attractive upgrade path for energies near 1.3 GeV.

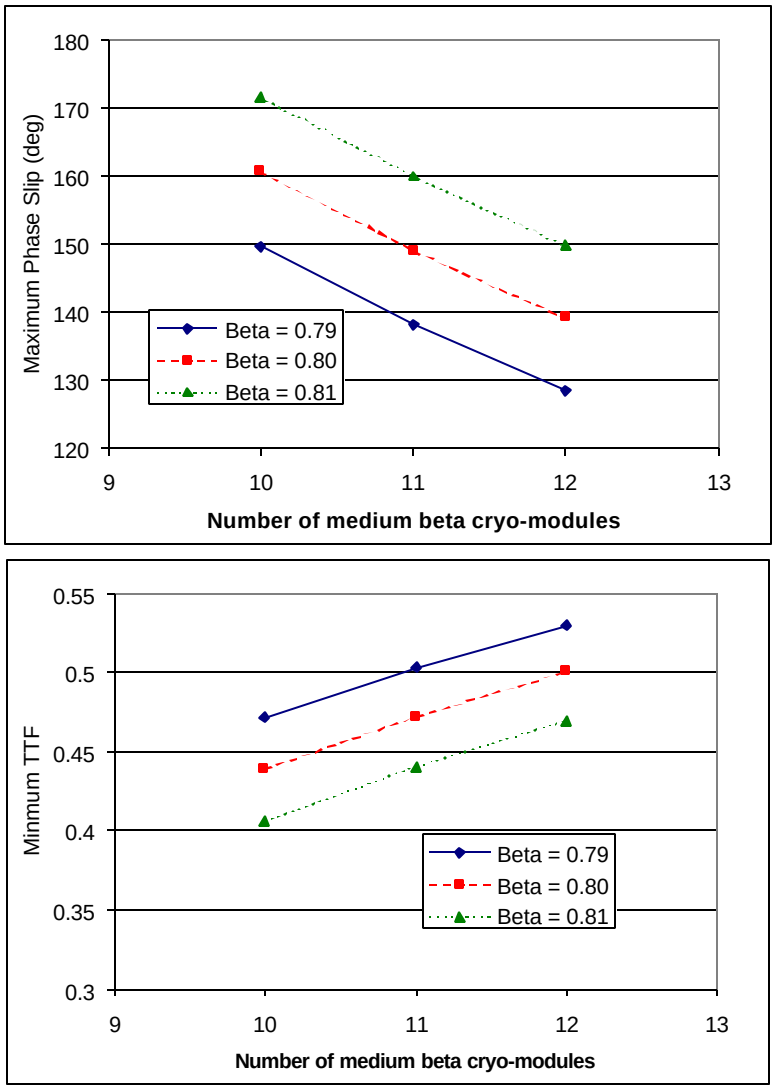

Figure 5. Maximum phase slip and minimum transit time factor (TTF), which occur in the first high beta cavity.

III Beam dynamics

Multi-particle beam dynamics in the linac are performed with the parmila code [3]. Particle input is taken from the exit of the RFQ, and tracked through a Medium Energy Beam Transport (MEBT) section, a DTL, section, a CCL section, and the superconducting cavity sections. Results are presented for cases both with and without errors (see Table 2). The resulting RMS transverse emittances throughout the linac are shown in Fig. 6. The influence of errors introduces a slight (~ 20%) emittance increase for the choice of errors used here. The jump in emittance at $\beta = 0.55$ is at the transition from the CCL to the superconducting region. In addition to the beam spot size from the emittance shown here, there is expected to be an effective beam size increase from the dynamic beam jitter due to vibrations in the DTL drift tube stems. This spot size jitter is estimated to be < 0.25 mm.

Table 2. Errors used in linac beam dynamics.

	Units	MEBT	DTL	CCL	SRF
Quad Errors:					
Displacement	cm	--	--	--	--
Pitch & yaw	deg	0.57	0.57	0.57	0.57
Roll	deg	0.25	0.29	0.29	0.29
Gradient	%	1.73	0*	0.5	0.5
Cavity Errors, Static	--	--	--	--	--
Cavity Errors, Dynamic					
Phase	Deg	0.5	0.5	0.5	0.5
Amplitude	%	0.5	0.5	0.5	0.5
Tilt	%	--	0.1	0.	0.

* Equivalent to 2% sorted.

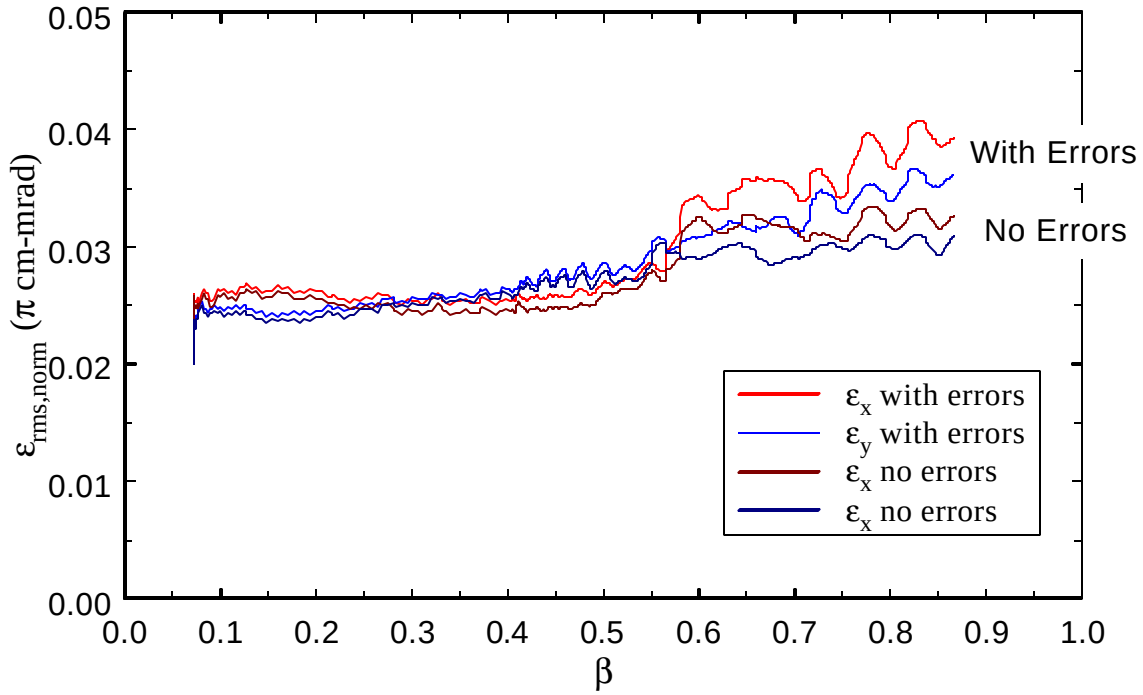

Figure 6. Transverse RMS emittance throughout the SNS linac, with and without errors.

References

[1] SNS, http://www.sns.gov/

[2] John Galambos, Jeff Holmes, Dong-o Jeon, and David Olsen , Synchronous Particle Scoping Studies for an SNS SC Linac, ORNL SNS Accelerator Physics Internal Memo, 9/14/99.

[3] H. Takeda, J. Billen, "Parmila", LANL report LA-UR-98-4478, (Feb. 2000).